

LIQUEFACTION MITIGATION MEASURES OF FINE SAND USING CEMENT GROUT UNDER CYCLIC LOADING

Arpit Jain

Research Scholar, Department of Civil Engineering
Indian Institute of Technology, Roorkee, India
E-mail: arpitjaintkg@gmail.com, ORCID: 0000-0002-7220-4040

Satyendra Mittal (Corresponding Author)

Professor, Department of Civil Engineering,
Indian Institute of Technology, Roorkee, India
E-mail: satyendramittal@gmail.com, ORCID: 0000-0001-6216-9205

Tshering Cheki

PG Student, Department of Civil Engineering
Indian Institute of Technology, Roorkee, India
E-mail: tsheringchokey143@gmail.com

ABSTRACT

The liquefaction phenomenon has been widely discussed and investigated due to its devastating outcomes. The triggering of liquefaction can be delayed through the significant ground improvement techniques like use of nano materials, epoxy impregnation, binder material etc. One the most effective, less costly and locally available OPC 43 (ordinary portland cement) can be tremendously helpful in the mitigation process for small to big projects of geotechnical engineering. The present study aims to observe the deformation characteristics of fine sand in terms of generated pore pressure, shear modulus and deviator stress at significant points. Twelve nos. strain controlled undrained cyclic triaxial tests were performed on both the non-grouted and cement grouted fine sand for the comparison. The tests conducted on fine sand treated with OPC 43, indicated that there is reduction in excess pore water pressure and enhancement of the stiffness degradation parameter. The tests were performed at two different relative densities of 35% and 65%, replicating loose and medium dense specimens, respectively. It has also been observed that after cement grouting, the number of cycles to reach initiation of liquefaction increased from 15 to 26.

KEYWORDS: Liquefaction, Cyclic loading, Cyclic triaxial test, Cement grouting

INTRODUCTION

Liquefaction phenomenon of sand can lead to loss of soil's bearing capacity, occurrence of ground subsidence, floating of embedded structures, lateral displacement of slopes and retaining walls, settlement of embankments, etc. The most dramatic cause of destruction has been the development of liquefaction in saturated sand deposits during an earthquake as evident either by the formation of sand boils and mud spouts at the ground surface or seepage of water through ground cracks as observed in Niigata earthquake [1]. Such occurrence is the trademark of all liquefaction phenomenon of saturated sand generated by earthquake loadings which cause tremendous destruction to engineering structures during an earthquake [2]. The relative density, stress history, particle size and shape, gradation of sand, nature of cyclic loading are the critical factors that determine liquefaction susceptibility. Hence the catastrophic nature of this type of failure has sparked the interest of many researchers and considerable work has been done to evaluate liquefaction susceptibility. Seed and Idriss [1] reported that in case of loose sand, the initial liquefaction and complete liquefaction occur simultaneously. However, there has been an increase in the magnitude of deviator stress required to cause liquefaction with an increase in relative density and for dense sand specimen, there is a considerable increase in the number of cycles required to cause liquefaction. The soil liquefaction phenomenon and factors affecting liquefaction have been studied by Florin and Ivanov [3], Prakash and Gupta [4] and Seed and Idriss [5].

To reduce the risk of liquefaction, improving soil condition has attracted the attention of many geotechnical engineers. Soil improvement methods like chemical grouting, densification, compaction grouting are most commonly employed to lessen or eliminate the effects of liquefaction. As observed by Rodriguez et al. [6] the chemical grouting found to be effective in reducing the liquefaction potential of sands. Here, the colloidal silica was selected as a stabilizing material which increased the resistance of untreated sands towards liquefaction. The different ground improvement techniques like dynamic compaction, vibroflotation have been adopted by previous researchers in order to enhance the condition of ground for usable purposes [7], [8]. Baker [9], Baez and Henry [10], Salley et al. [11] described the use of compaction grouting to treat liquefiable sands. The test results show that the values of CPT tip resistances had increased from an average of about 2.3 MPa before treatment to an overall average of about 7.9 MPa. Vipulanandan and Ata [12] studied the behavior of silicate grouted sand using cyclic triaxial compression test performed at load-controlled condition and observed that the grouted sand failed below an axial strain of 0.3% and the damping ratio of grouted sand varied between 2 and 4% during the initial loading cycles. Though widely used, traditional mitigation methods such as densification, drainage, dewatering, etc. have limitations like environmental impact, disturbance to existing and neighboring structures when subjected to vibrations, etc. Soil improvement technique with neat cement grout can be an encouraging solution to enhance the liquefaction resistance of vulnerable soil. The grouting has the following advantages a) treatment can be done beneath existing structures, b) treatment in areas where low levels of vibration and noise were required, c) treatment of even narrow areas. Porcino et al. [13] investigated the behavior of lightly grouted loose medium sand under both monotonic and cyclic loading and that the weak cementation level induced by chemical treatment was sufficient to moderately increase small-strain stiffness. Porcino et al. [14] performed an experimental study on the silicate- grouted sand where the influence of loading mode on undrained cyclic strength behavior is compared for both treated and non-treated specimens. Here, the effect of curing time and loading frequency were also explored. The strength of cemented sand is investigated through experimental characterisation and numerical simulation where the dilatancy at the peak state increases with increasing cement content [15]. Gallagher et al. [16] found out the influence of colloidal silica grout on the liquefaction potential of loose sand, also the cyclic undrained characteristics observed to be significantly different due to the presence of grout. The dynamic soil properties have been significantly affected after the improvement techniques, this is due to the reduction in degradation characteristics. Choobbasti et al. [17] observed the effect of nanosilica and cement on sandy soil by performing the static and cyclic triaxial tests. By varying the percentage of nano-silica and cement the changes in dynamic deformation modulus, damping ratio and shear strength properties of sandy soil were observed. The chemical grouting has significant effect on the dynamic soil properties of sand in both the low and high strain conditions [[18], [19], [20]]. In most of the previous studies, the grouting mechanisms were significantly increasing the liquefaction resistance in both the field and laboratory tests. Most of the research work was related to silica grout and other chemical grouts for the improvement in degradation characteristics. In this particular study, cement grout was chosen, as it is cost effective and easily available in local markets. Also, the strain controlled tests provide the most critical failure stress at a particular strain value.

This paper presents the results of cyclic triaxial strain-controlled tests where cyclic loading were provided on the reconstituted specimens of fine sand and cement grouted composite. The pore pressure behavior, deviator stress and dynamic soil properties change significantly after grouting with cement slurry. The variation in the pore pressure response of soil-cement composite affected the shear modulus, characteristics of load vs deformation curve and liquefaction resistance at two different densities.

MATERIALS

1. Sand Used

The fine sand used was obtained from the bed of Solani river located in Roorkee (Uttarakhand), India and classified as poorly graded sand (SP) as per IS classification [21]. The sand used in the test was cleaned and oven-dried before starting tests. Figure 1 shows the grain size distribution curve of the sand used in the test and Table 1 gives its other index properties.

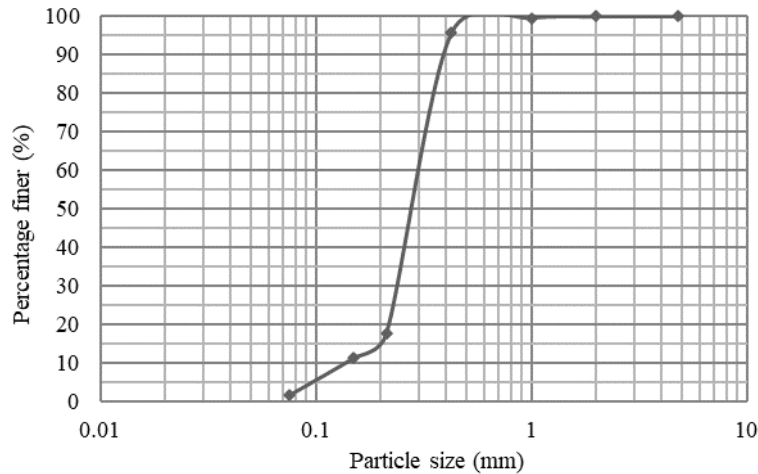


Fig. 1 Grain size distribution curve of fine sand

Table 1: Properties of fine sand

Sl. No	Particulars	Notations	Value
1	Soil type	SP	Poorly graded soil
2	Specific gravity	G	2.63
3	Coefficient of uniformity	C_u	2.51
4	Coefficient of curvature	C_c	1.44
5	Effective grain Size (mm)	D_{60}	0.32
		D_{30}	0.24
		D_{10}	0.13
6	Maximum void ratio	e_{max}	0.79
7	Minimum void ratio	e_{min}	0.56

2. Grouting Material Used

The cement grout used in the study was a mixture of 43 Grade Ordinary Portland cement (OPC 43) and water in the ratio of 1:3 (cement: water) by weight. This mix is cost-effective and also has less potential for toxicity. After performing several preliminary tests on a shake table, this particular cement: water ratio of 1:3 was adopted as an optimum content as a mitigation against liquefaction. Therefore, cyclic triaxial tests were performed at this ratio. Table 2 provides the chemical contents and the basic physical properties of cement.

Table 2: Properties of 43 Grade Ordinary Portland cement

Sl. No	Properties	Description
1	Specific gravity	3.16
2	Consistency	33%
3	Setting time	Initial setting time = 55 minutes Final Setting time = 312 minutes
4	Fineness	5.32%
5	Compressive strength	43 MPa
6	Chemical composition	$SiO_2, Al_2O_3, Fe_2O_3, MgO, CaO, Na_2O, K_2O, MnO, TiO_2$ and P_2O_5

EXPERIMENTAL SET UP

1. Cyclic Triaxial Apparatus

Fully computerized cyclic triaxial system, with the capability of performing both static and dynamic testing was used in this particular study. During dynamic testing, both stress and strain controlled techniques could be used in this machine. The whole cyclic triaxial machine consists of the load cell,

Linear Variable Differential Transformer (LVDT) and transducers to detect pore water pressure, volume change, and lateral deformations. The triaxial cell with low friction piston rod, along with a 10 kN servo controlled submersible load cell. The loading system consists of a load frame and a hydraulic actuator with a capability of performing both strain and stress-controlled tests (by servo-hydraulic loaders) at a wide range of frequency from 0.1 Hz to 5 Hz. In this particular study, frequency used as 1 Hz for the cyclic loading was provided. Figure 2 shows the image of cyclic triaxial apparatus with suitable detailing.

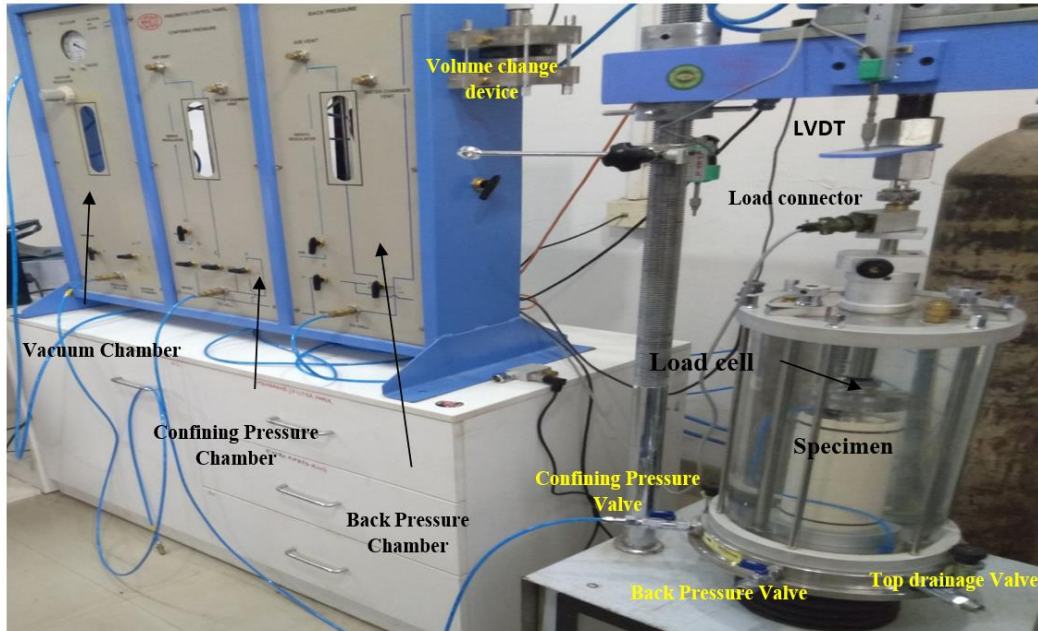


Fig. 2 Cyclic triaxial testing facility

2 Specimen Preparation in Cyclic Triaxial Apparatus

The specimens having dimensions 70 mm diameter and 140 mm height were prepared for both the non grouted and cement grouted sand. In the present study, dry pluviation method was adopted as the specimen preparation technique as suggested by Ladd [22]. Oven dried sand was filled by maintaining a constant fall height using a cone-shaped funnel into the mold as shown in Figure 3. The funnel tube is of about 25 mm diameter placed at the bottom of the membrane-lined split mold. Plastic pipes of about 8 mm diameter and 150 mm length were placed inside the cylindrical split mold of size 70 mm dia and 140 mm height, for the preparation of grouted sand specimens for cyclic triaxial tests. In order to prepare specimen, the first step was to fix up the membrane inside the split-mold using applied vacuum. Then, three grout pipes were placed vertical at a predetermined location from the geometry. The calculated amount of sand was placed inside using a tube connected to the conical funnel. The tube raised upwards carefully after maintaining a constant fall height. The prepared cement slurry was poured using grout pipes with constant upward movement with full precision. In order to complete the curing process, the specimen left for 24 hrs. Three pipes in a triangular pattern were used. In case of grouted sand, pipes were installed earlier to fill cement slurry. Then, sand was poured using the dry pluviation technique as shown in Figure 3. The sand was poured in three stages and after each stage slight compaction was given with the help of a tapping rod [23] without affecting the required density. Then, the process of filling cement slurry started where pipes were pulled up slowly for the recovery of plastic pipes. Finally after ensuring that slurry has reached the surface, specimen was trimmed at the top of the mold and after placing filter paper and porous stone, the triaxial cell was installed. After the completion of curing time, the split mold was then removed and triaxial cell mounted and then next process of saturation started. A small vacuum of about 15 kPa was applied to the specimen for the verticality of the sand specimen. Figure 4 shows a schematic diagram for the specimen preparation. The pictorial representation of grouting location is shown in Figure 5.



Fig. 3 Sample preparations using dry pluviation method

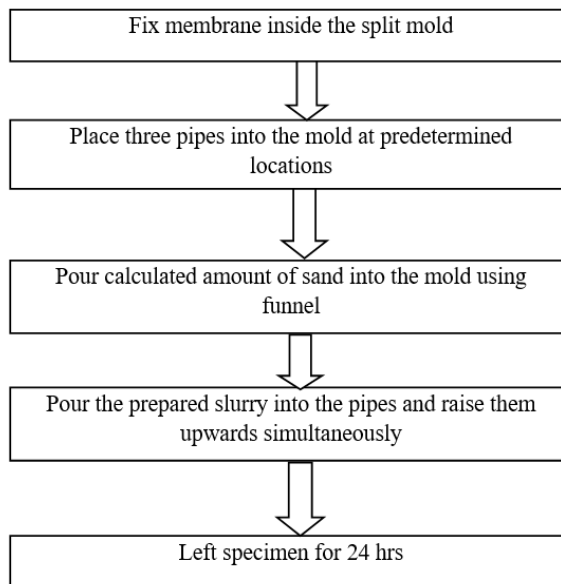


Fig. 4 Procedure of specimen preparation

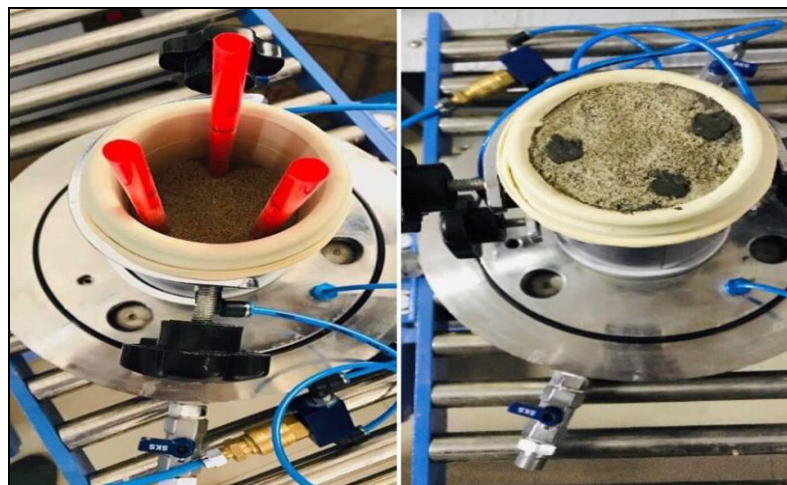


Fig. 5 Pictorial representation of grouting locations

3. Saturation, Consolidation and Loading stages

The specimens prepared were then saturated with de-aired water using back pressure saturation. In order to expedite the saturation process, the specimen was flushed with carbon dioxide (CO₂) for 10-15 minutes with the initial cell pressure of 50 kPa. Subsequently, de-aired water was passed through the CO₂ flushed specimen. To attain saturation, the cell pressure and back pressure were then gradually increased in stages while maintaining almost constant pressure of about 20 kPa. This process was continued until the Skempton's pore pressure parameter i.e. $B = \Delta u / \Delta \sigma'_3$ (Δu is the change in specimen pore pressure and $\Delta \sigma'_3$ is the change in confining pressure) exceeds 0.95. After saturation, the specimens were isotropically consolidated at an effective confining pressure of 100 kPa. The volume change of specimens during consolidation was recorded by the sensitive volume measuring device. Once the consolidation process had completed, the specimens were subjected to undrained shearing under sinusoidal cyclic loading at a strain rate of 0.4%. Before deciding the rate of axial strain, several trial tests were also performed at a strain rate of 0.2%, 0.4% and 0.6%. At a strain rate of 0.2% the changes in pore pressure were less significant for the analysis while at a strain rate of 0.6% , the generated strains were too quick to follow. Therefore, 0.4% strain rate was chosen as an ideal strain rate.

TEST RESULTS AND ANALYSIS

Total 12 nos. strain-controlled cyclic triaxial tests were performed on the isotropically consolidated specimens of fine sand. The summary of tests series has been presented in Table 3. Each test specimen was subjected to 100 cycles of sinusoidal strain-controlled loading. In order to maintain the uniformity in results, the analysis part was considered for 55 cycles as most of the trends are not significant after these number of cycles. Also, for the representation, analysis of four tests U_L3, T_L6, U_M9 and T_M12 are chosen. This study is corresponding to the axial strain of 0.4% subjected to sinusoidal waveform (frequency =1 Hz) on soil.

Table 3: Summary of performed tests on tested materials

Test No.	The specimen	D_r	N_f
1	U_L1	35%	15
2	U_L2	35%	16
3	U_L3	35%	16
4	T_L4	35%	20
5	T_L5	35%	22
6	T_L6	35%	20
7	U_M7	65%	25
8	U_M8	65%	26
9	U_M9	65%	25
10	T_M10	65%	27
11	T_M11	65%	26
12	T_M12	65%	26

U: Untreated, *T*: Treated, *L*: Loose soil, *M*: Medium dense, D_r : Relative Density , N_f : Number of cycles required for the initiation of liquefaction

1. Variations in Pore Water Pressure Ratio Corresponding to Density and Grouting Behavior

In this study, improvement technique using grouting mechanism was chosen on fine sand. As the number of cycles increases, there was a generation of excess pore water pressure which ultimately causes the liquefaction of soil specimen. This generated pore water pressure plays a key role in the failure of the soil system. A comparative study on the cement grouted and non grouted soil using pore water pressure ratio is presented in Table 4 for two different relative density (D_r). The increment in pore pressure ratio (r_u) to unity was considered as the initiation of liquefaction by Seed and Lee [24].

$$r_u = \frac{\Delta U}{\sigma'_{3c}} \tag{1}$$

where r_u = pore pressure ratio, U = Pore Pressure, σ'_{3c} = initial effective confining stress

The variation in pore pressure ratio for the specimens U_L3 and T_L6 is depicted in Figures 6 and 7, respectively. The maximum r_u value observed is 1.18 (Table 4) which can be considered as the liquefied state. The results of maximum r_u values for different specimens are tabulated in Table 4. After treatment with cement slurry at same D_r as performed in the specimen T_L6, maximum r_u value reduced to 1 (Table 4). This was due to the replacement of soil particles with cement slurry at some specific zones. On increasing the density to 65% in specimen U_M9 the percentage decrease in r_u was observed as 22% as compared to specimen U_L3 (Figure 8). In the specimen T_M12, the treatment with cement slurry affected the soil structure where the maximum r_u reached as 0.72 as shown in Figure 9. Here the effect of both density and grouting played a key role in diminishing the excess pore water pressure.

Table 4: List of maximum r_u values for the tested grouted and non grouted specimens

Specimen number	D_r	Maximum r_u
U_L3	35%	1.18
T_L6	35%	1
U_M9	65%	0.92
T_M12	65%	0.72

r_u : Pore pressure ratio, D_r : Relative density

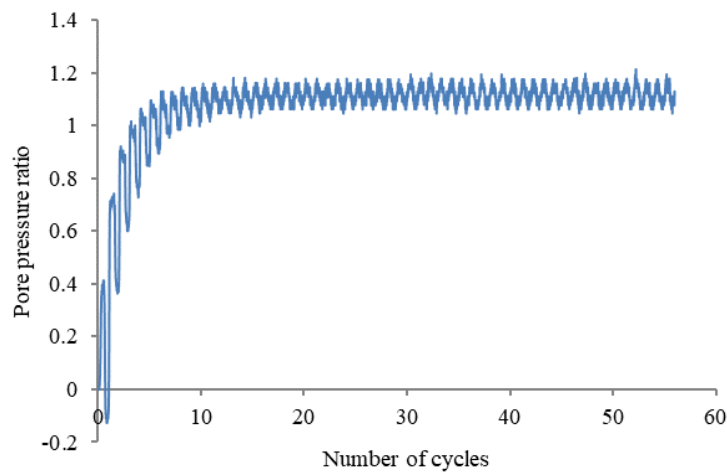


Fig. 6 Pore pressure ratio vs number of cycles for the specimen U_L3

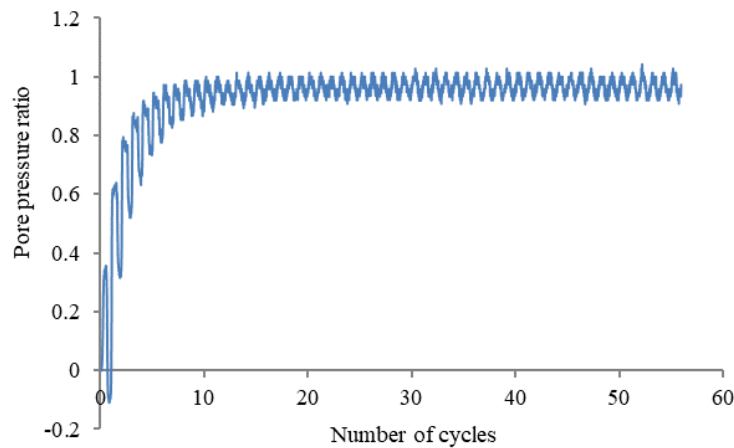


Fig. 7 Pore pressure ratio vs number of cycles for the specimen T_L6

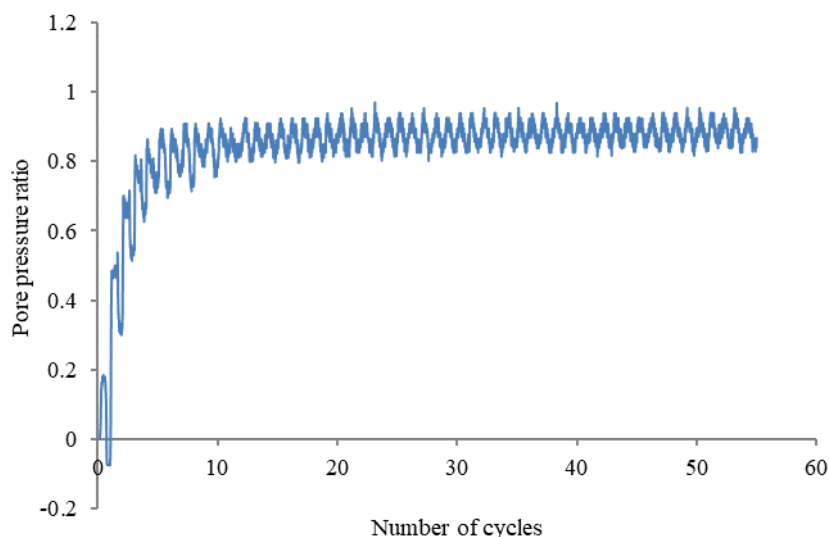


Fig. 8 Pore pressure ratio vs number of cycles for the specimen U_M9

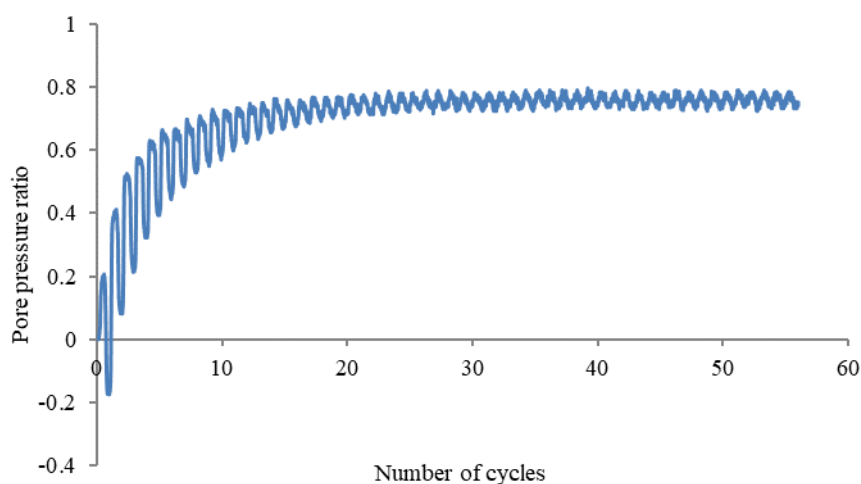


Fig. 9 Pore pressure ratio vs number of cycles for the specimen T_M12

The phenomenon of liquefaction is clearly visible in the specimen U_L3 due to the less dense specimen at an D_r of 35% where the N_f value obtained is 16 (Table 3). Due to the presence of cement slurry, more load is transferred to cement soil composition which resulted in the decrement of excess pore water pressure development as occurred in the specimen T_L6, initiation of liquefaction observed here at 20th cycle (Table 3). Meanwhile more dense specimen like U_M9 has performed better than grouted one which is due to increased grain to grain load transfer. Here, the improvement was achieved by densifying the specimen, N_f value observed as 25 while N_f value was 26 for the specimen T_M12. This slight variation in N_f values in the specimens U_M9 and T_M12 shows that grouting has a very little effect on time to reach liquefaction initiation for medium dense specimen as observed.

2 Behaviour of Load vs Deformation Curve on Cement Grouted and Non-Grouted Specimens

As shown in Figures 10 to 13, a graphical representation of load vs deformation is presented for the specimens of varying density and grouting behavior. The cementation can be helpful in the increment of liquefaction resistance of sand as observed by Clough et al. [25], Reddy and Saxena [19]. In the specimen U_L3, the maximum load carried out was 21 kg as shown in Figure 10 while specimen T_L6 carried the maximum load as 22 kg (Figure 11). As it can be easily observed in the specimens U_L3 and T_L6, the

effect of grouting is not useful to carry the load which can be due to the less curing time period of 24 hours, resulted in less strength development of cement slurry. When cyclic loading applied on medium dense specimen U_M9, the maximum load sustained at 25 kg as shown in Figure 12. Specimen T_M12 sustained at even 1.28 times the maximum load of the specimen U_M9.

The cement grout becomes more load resistive due to the hardening of calcium silicate which causes the rise in the load carried by treated specimens. The grouting was effective in the reduction of excess pore water pressure development as explained in section 4.1. In the specimens U_M9 and T_M12, the effect of grouting is observed in order to enhance the load carrying capacity of the specimen at medium dense condition. The pattern of load vs deformation curve obtained is nearly same for the specimens U_L3 and T_L6. But this pattern of T_L12 is different due to the difference in particle arrangement in medium dense specimens.

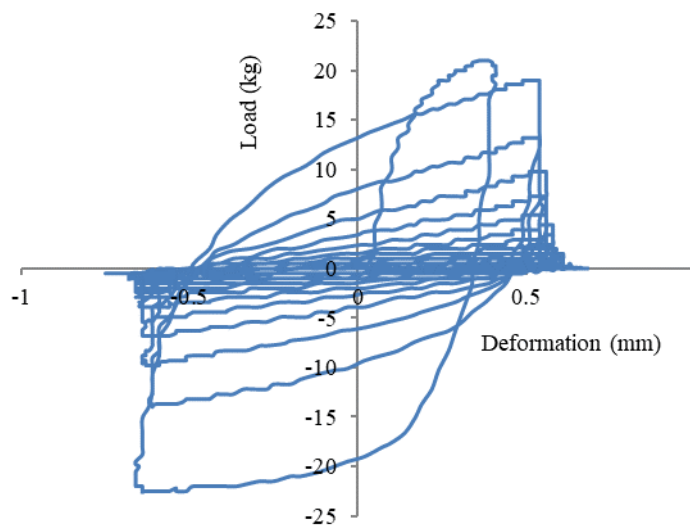


Fig. 10 Load vs deformation curve for the specimen U_L3

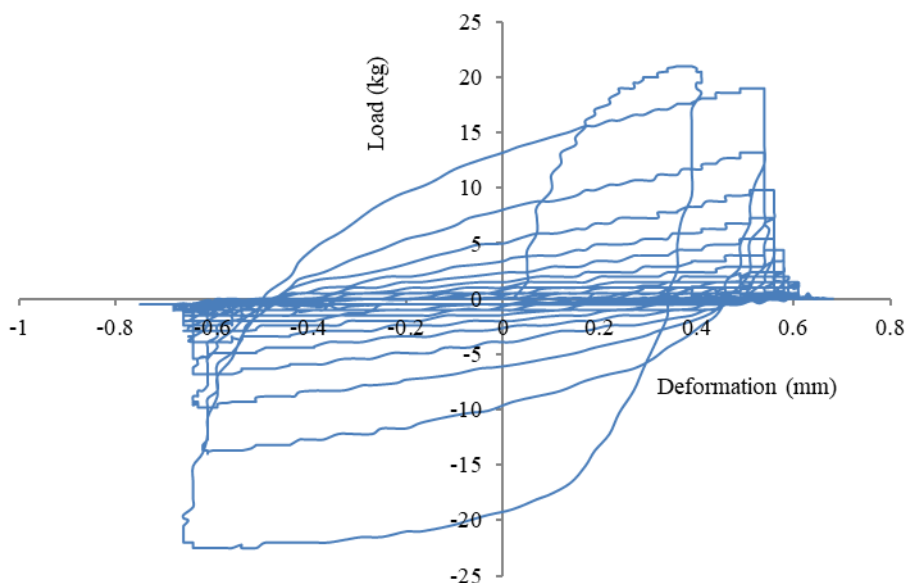


Fig. 11 Load vs deformation curve for the specimen T_L6

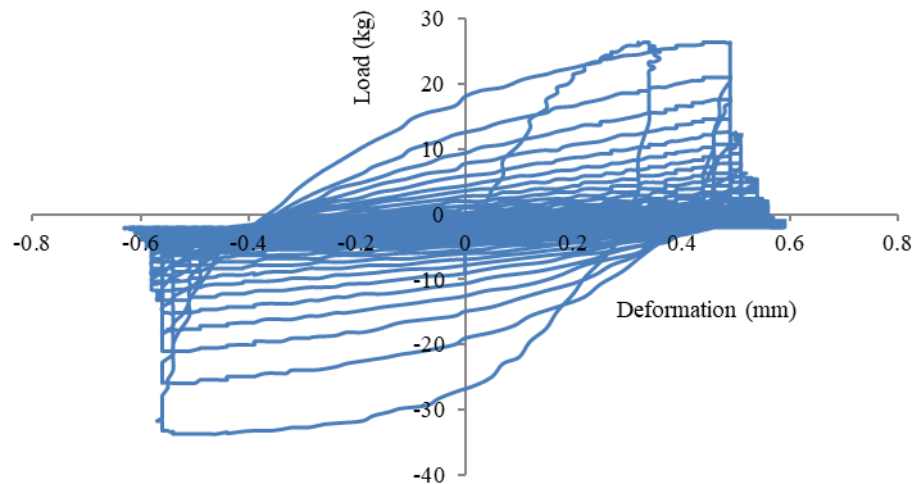


Fig. 12 Load vs deformation curve for the specimen U_M9

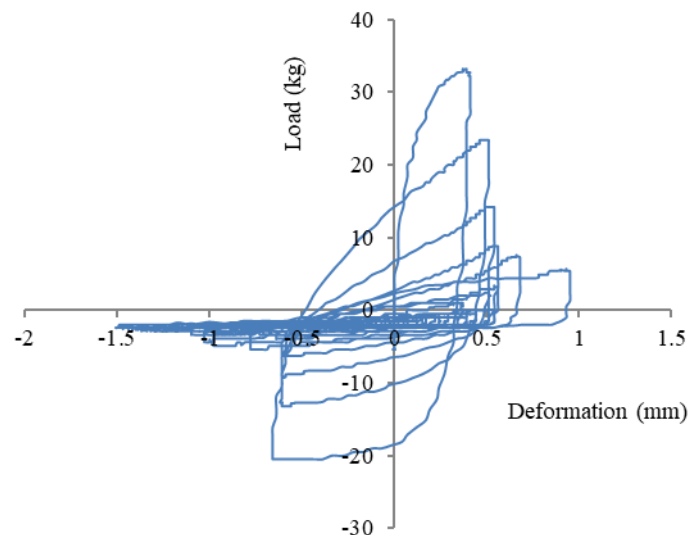


Fig. 13 Load vs deformation curve for the specimen T_M12

3. Variations in Shear Modulus for Cement Grouted and Non-Grouted Specimens

Shear modulus is a parameter of stiffness degradation. Figure 14 depicts the pattern of shear modulus (G) for the specimens U_L3, T_L6, U_M9, and T_M12. Grouting of cement slurry imparts the stiffness in soil matrix which results in the increment of degradation characteristics. This causes the enhancement in shear modulus values of soil-cement composite. The dynamic properties of untreated and the cemented sand were observed at low strain by Saxena et al. [26], Baig et al. [27] and Acar et al. [29]. Maher et al. [18] performed series of resonant column and cyclic triaxial tests on the sand specimens treated with sodium silicate grout. Here, the significant advancement was observed in the shear modulus of the tested sand due to the formation of stiff gels.

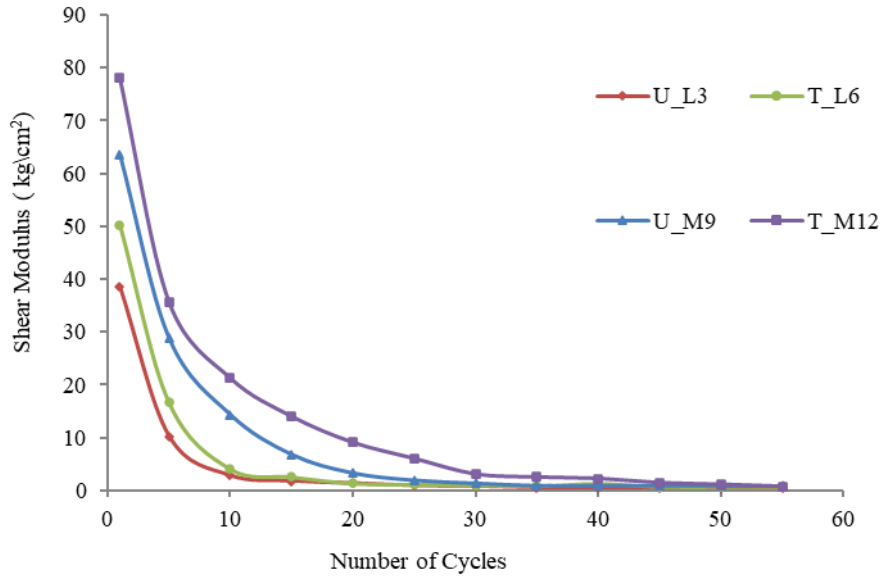


Fig. 14 Variation of shear modulus for the specimens U_L3, T_L6, U_M9 and T_M12

As cyclic loading applied to the specimen, there was a generation of excess pore water pressure which ultimately diminishes effective stress. Due to hardening of calcium silicate there was less degradation in more dense and grouted specimens as shown in Figure 14. For the specimens U_L3, T_L6, U_M9 and T_M12, maximum G values obtained are 38.66, 50.23, 63.63, 78 (all in kg/cm²) respectively.

Plots obtained against shear modulus and numbers of cycles are of the same pattern for the different specimens. The changes are observed in the calculated G values due to the density and presence of cement slurry grouting where stiffness is certainly enhanced. After 55 cycles most of the specimens had degraded which causes the specimens to attain nearly the same values of shear modulus as 0.4716, 0.7112, 0.8281 and 0.7729 which shows the significant degradation of soil cement composite.

4. Behaviour of Deviatoric Stress vs Time Curve for Changes in D_r on Cement Grouted and Non-Grouted Specimens

Figures 15 to 18 show the plots of deviatoric stress vs time for the specimens U_L3, T_L6, U_M9, and T_M12. Peak deviator stress (q_{max}) values corresponding to U_L3, T_L6, U_M9 and T_M12 are presented in Table 5. The deviatoric stress value enhanced for higher density but for the specimens U_L3 and T_L6, q_{max} value was nearly same because the curing time considered as 24 hours which resulted in less strength increment meanwhile excess pore water pressure generation was countered by grouting of the specimens even at the same density. The specimen T_M12 took more load as compared to non grouted specimen U_M9.

Table 5: List of q_{max} values on grouted and non grouted specimens

The specimen	D_r	q_{max} (kg/cm ²)
U_L3	35%	0.42
T_L6	35%	0.45
U_M9	65%	0.53
T_M12	65%	0.60

q_{max} : Peak deviatoric stress (kg/cm²), D_r : Relative density

The patterns obtained were nearly same for U_L3 and T_L6 (Figures 15 and 16) while the specimens U_M9 and T_M12 failed in the tensile zone which can be clearly observed from Figures 17 and 18. The pattern of the figures obtained is nearly the same for the specimens U_L3 and T_L6. Also these are nearly symmetric about the x-axis (deformation) which can be seen in Figures 15 and 16.

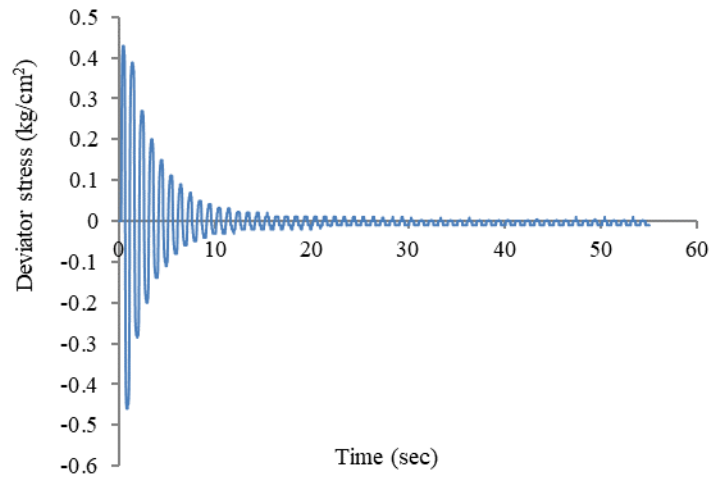


Fig. 15 Deviatoric stress vs time plot for the specimen U_L3

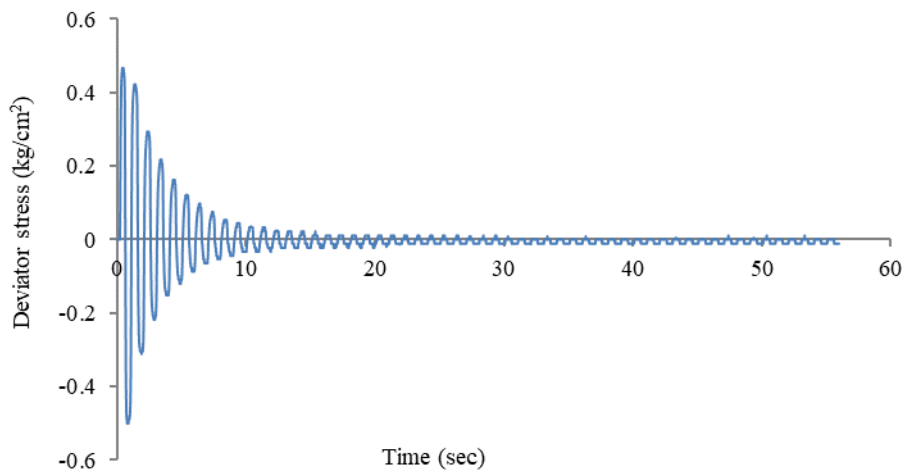


Fig. 16 Deviatoric stress vs time plot for the specimen T_L6

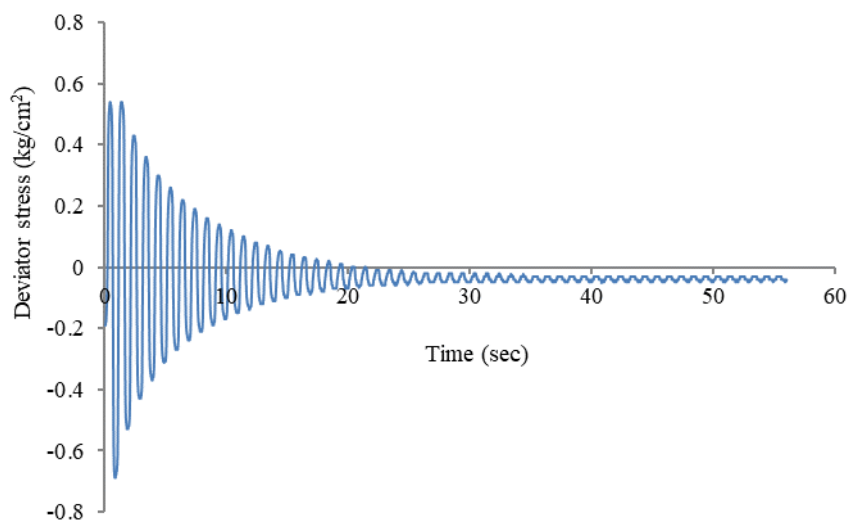


Fig. 17 Deviatoric stress vs time plot for the specimen U_M9

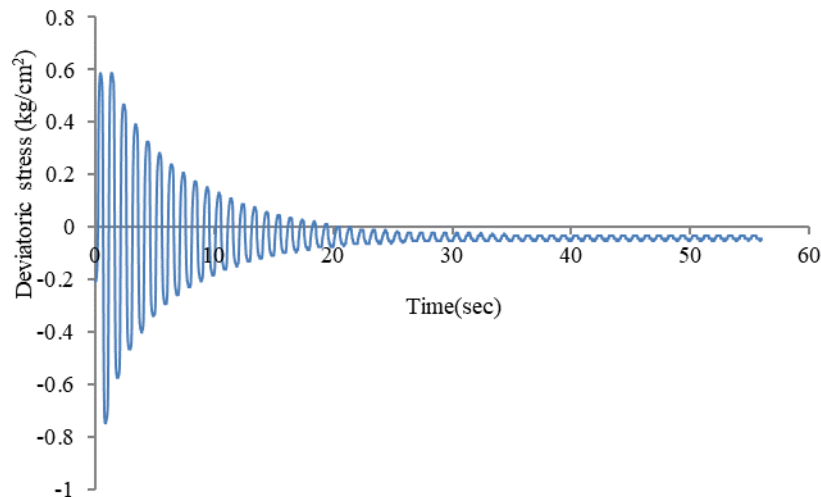


Fig. 18 Deviatoric stress vs time plot for the specimen T_M12

5. Comparison with Previous Study

The results of the present study have been compared with the study of Porcino et al. [29]. The moderately cemented grout was used by Porcino et al. [29] for the mitigation of liquefaction. The present study shows that medium dense sand treated with cement grout (in already defined proportion) got liquefied in 28 cycles at a CSR (cyclic stress ratio) of 0.43. Figure 19 shows the comparison between present study and that of Porcino et al. [29]. This projects the mitigating effect of cement grout used.

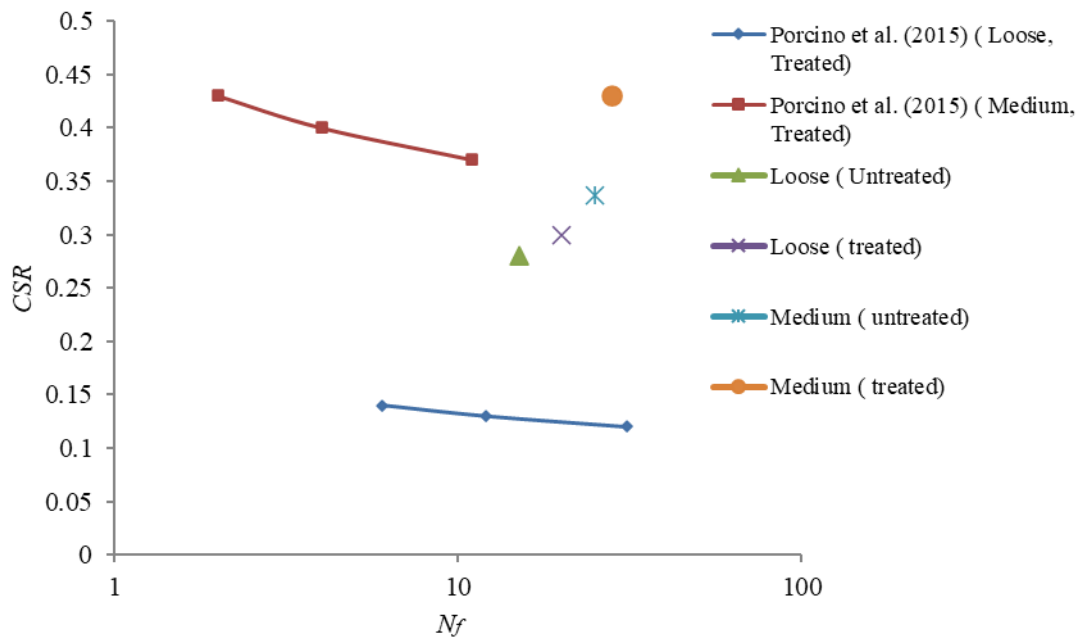


Fig. 19 CSR vs N_f (number of cycles required for liquefaction)

CONCLUSIONS

Undrained cyclic triaxial tests had been performed on fine sand to study the effect of density on cement grouted and non-grouted soil specimens. Grouting mechanism was effective in the reduction of liquefaction phenomenon through less pore pressure development with increment in load carrying capacity. The cement slurry increased the shear modulus of soil to 2.01 times as compared to that of the untreated soil specimen. The major findings from the current study are summarized below:

- a) Maximum r_u value was 1.18 as observed in U_L3 specimen with D_r as 35%, , which further reduced to 0.72 in T_M12 specimen having relative density of 65%.
- b) As observed in this study, grouting had less effect on the time to reach liquefaction initiation for medium dense specimen. The key role played by density and cement grouting increased the peak deviatoric stress value in specimen T_M12 to 1.42 times than that of the U_L3 specimen. Also, grouting was not much effective to increase q_{max} value at low density but satisfactory results were obtained at the medium density.
- c) The final value of shear modulus after degradation in all the specimen was 0.711 or nearby. Shear modulus (G) attained a higher value of 78 kg/cm² for the medium dense grouted specimen (T_M12) when compared with the loose non-grouted specimen (U_L3) with a G value of 38.66 kg/cm².

REFERENCES

1. Seed, H.B. and Idriss, I.M. (1967). "Analysis of Soil Liquefaction Niigata Earthquake", *Journal of Soil Mechanics and Foundation Division*, Vol. 93, No. 3, pp. 83-108.
2. Kramer, S.L. (1996). "Geotechnical Earthquake Engineering", *New Jersey: Prentice Hall, Upper Saddle River*.
3. Florin, V.A. and Ivanov, P.L. (1996). "Liquefaction of Saturated Sandy Soils", *Proceedings of the 5th International Conference on Soil Mechanics and Foundation Engineering, Paris, Vol. 1, pp. 107-111*.
4. Prakash, S. and Gupta, M.K. (1970). "Blast Test for Tenughat Dam Site", *Journal of South East Asian Society of Soil Engineering*, Vol. 1, No. 1, pp. 41-50.
5. Seed, H.B. and Idriss, I.M. (1971). "Simplified Procedure for Evaluating Soil Liquefaction Potential", *Soil Mechanics and Foundation Division*, Vol. 107, No. 9, pp. 1249-1274.
6. Rodriguez, J.A.D. and Izarraras, V.M.A. (2004). "Mitigation of Liquefaction Risk using Colloidal Silica Stabilizer", *In: 13th World Conference on Earthquake Engineering Vancouver, B.C., Canada*.
7. D'Appolonia, E., Miller, C.E. and Ware, T.M. (1954). "Sand Compaction by Vibroflotation", *Transactions ASCE*, Vol. 154.
8. Mayne P.W., Jones J.S. and Dumas, J.C. (1984). "Ground Response to Dynamic Compaction", *Journal of Geotechnical Engineering*, Vol. 110, pp. 757-774.
9. Baker, W.H. (1985). "Embankment Foundation Densification by Compaction Grouting", *Proceeding issues in Dam grouting, New York, ACSE, 104-122*.
10. Baez, J.I. and Henry, J.F. (1983). "Reduction of Liquefaction Potential by Compaction Grouting at Pinopolis West Dam", *Geotechnical practice in dam rehabilitation New York*.
11. Salley, J.R., Foreman, B., Baker, W. and Henry, J.F. (1987). "Compaction Grouting Test Program Pinopolis West Dam", *Proceedings of Soil improvement - A 10-year update, New York, pp. 245-269*.
12. Vipulanandan, C. and Ata, A. (2000). "Cyclic and Damping Properties of Silica-Grouted Sand", *Journal of Geotechnical and Geoenvironmental Engineering*, Vo. 126, No. 7, pp. 650-656.
13. Porcino, D., Marciano, V. and Granata, R. (2012). "Static and Dynamic Properties of a Lightly Cemented Silicate-Grouted Sand", *Canadian Geotechnical Journal*, Vol. 49, pp. 1117-1133.
14. Porcino, D., Marciano, V. and Granata, R. (2011). "Undrained Cyclic Response of a Silicate-Grouted Sand for Liquefaction Mitigation Purposes", *Geomechanics and Geoengineering*, Vol. 6, No. 3, pp. 155-170.
15. Wang, Y.H. and Leung, S.C. (2008). "Characterization of Cemented Sand by Experimental and Numerical Investigations", *Journal of Geotechnical and Geoenvironmental Engineering*, Vol. 134, No. 7, pp. 992-1004.
16. Gallagher, P.M. and Mitchell, J.K. (2002). "Influence of Colloidal Silica Grout on Liquefaction Potential and Cyclic Undrained Behavior of Loose Sand", *Soil Dynamics and Earthquake Engineering*, Vol. 22, pp. 1017-1026.
17. Choobasti, A.J., Vafaei, A. and Kutanaei, S.S. (2018). "Static and Cyclic Triaxial Behavior of Cemented Sand with Nanosilica", *J. Mater. Civ. Eng.*, Vol. 30, No. 10, pp. 04018269.

18. Maher, M.H., Ro, K.S. and Welsh, J.P. (1994). "High Strain Dynamic Modulus and Damping of Chemically Grouted Sand", *Soil Dynamics and Earthquake Engineering*, Vol. 13, No. 2, pp. 131-138.
19. Reddy, K.R. and Saxena, S.K. (1992). "Liquefaction Resistance of Cemented Sands under Multidirectional Cyclic Loading", *Canadian Geotechnical Journal*, Vol. 29, pp. 989-993.
20. Ribay, E.D., Maigre, I.D., Cabrillac, R. and Gouvenot, D. (2004). "Shear Modulus and Damping Ratio of Grouted Sand", *Soil Dynamics and Earthquake Engineering*, Vol. 24, No. 6, pp. 461-471.
21. IS:1498-1970, "Classification and Identification of Soils for General Engineering Purposes".
22. Ladd, R.S. (1977). "Specimen Preparation and Cyclic Stability of Sands", *J. Geotech. Engrg. Div*, Vol. 103, No. 6, pp. 535-547.
23. Ladd, R.S. (1978). "Preparing Test Specimens Using Undercompaction", *Geotech. Testing J.*, Vol. 1, No. 1, pp. 16-23.
24. Seed, H.B. and Lee, K.L. (1966). "Liquefaction of Saturated Sands During Cyclic Loading", *J. Soil Mech. and Found. Div*, Vol. 92, No. 6, pp. 105-134.
25. Clough, G.W., Iwabuchi, J., Rad, N.S. and Kuppusamy, T. (1989). "Influence of Cementation on Liquefaction of Sands", *J. of Geotech. Eng*, Vol. 115, No. 8, pp. 1102-1117.
26. Saxena, S.K., Avramidis, A.S. and Reddy, K.R. (1988). "Dynamic Moduli and Damping Ratios for Cemented Sands at Low Strains.", *Canadian Geotechnical Journal*, Vol. 25, pp. 353-368.
27. Baig, S., Picornell, M. and Nazarian, S. (1997). "Low Strain Shear Moduli of Cemented Sands", *Journal of Geotechnical and Geoenvironmental Engineering*, Vol. 123, No. 6, pp. 540-545.
28. Acar, Y.B. and El-Tahir, A. (1986). "Low Strain Dynamic Properties of Artificially Cemented Sand", *Journal of Geotechnical Engineering*, Vol. 112, No. 11, pp. 1001-1015.
29. Porcino, D., Marciano, V. and Granata, R. (2015). "Cyclic Liquefaction Behaviour of a Moderately Cemented Grouted Sand under Repeated Loading", *Soil Dynamics and Earthquake Engineering*, Vol. 79, pp. 36-46.